POAC'13
Espoo, Finland

Proceedings of the 22nd International Conference on
Port and Ocean Engineering under Arctic Conditions
June 9-13, 2013
Espoo, Finland

Reanalysis of Pressure Patterns and Pressure-Area Curves Considering Resolution of Pressure Measurement Film

Hyunwook Kim [1], Claude Daley [1]

[1]Memorial University, St.John's, Canada

ABSTRACT

Demand for resource development and transportation purpose in the arctic region induced many field tests and laboratory ice crushing tests performed since the 1970s. The main purposes of series of tests were to understand the ice behavior and measure the magnitude of ice load/pressure during ice-structure interaction. Resolution of the data measurement system is one of the important points to analyze the obtained data. The 'high-resolution' pressure measurement film was applied to obtain pressure distribution and magnitude of pressure. In a former study, only one optimized resolution was selected considering the quality of plots and effectiveness of the data process. In this study, different resolutions were selected and data process was performed to understand the effect of the resolution. Activated area, total force, pressure distribution and pressure-area curves were analyzed. As a result, optimal resolution was discussed.

INTRODUCTION

In laboratory ice crushing test, it is common that only a nominal area, which is obtained from 'controlled' crushing distance, and force data is available for the data analysis.

In previous studies, measuring 'real-time' basis contact area and pressure distribution was attempted using electronic devices or pressure panel system. However, due to the restricted resolution, rate of data acquisition, and difficulty of calibration, there were limits to be applied flexibly. Furthermore, recording real-time contact area and pressure distribution is highly sensitive to the data-acquisition system. Therefore, the level of measuring all phenomena occurring in an extremely short time is not sufficient due to a resolution and frequency of the data-acquisition system.

Many of the researchers start to recognize the importance of the resolution of the data measurement system. However, most of the field test data were acquired from different test condition, for example, ice condition and ambient temperature during the test. Therefore, direct comparison regarding to resolution between each test data is impractical.

Kim, Daley and Ulan-Kvitberg [1] applied 'chemical' pressure measurement film in laboratory scale test and 'activated' contact area and the pressure distribution was obtained.

The advantage of the pressure measurement film in laboratory ice crushing test is simplicity of application. Prior to ice crushing test, simply attach a pressure measurement film in any location where measuring a contact area and pressure distribution is required. Process of calibration of the film is well established. Furthermore, the film itself has high-resolution and response to applied loads without any delay.

In a previous study, all data analysis was performed solely on the one pixel size. It is a general idea that the result tends to be more accurate when the pixel size is getting smaller. However, too much data can cause excessive analysis time. Therefore, it is important to verify a proper pixel size for efficient data analysis.

In this study, an assessment of the effect of the pixel size was done by analyzing the same experimental data with various pixel sizes. For the comparison, 1) contact area, 2) total measured force, 3) overall pressure distribution, and 4) 'spatial' pressure-area curve were chosen as comparative assessment categories.

PRESSURE MEASUREMENT FILM

There are seven types of pressure measurement film from 'Extreme low' to 'Super high'. The film is categorized by a detectable pressure range. Prior to study, pre-tests were performed to identify the pressure ranges during an ice crushing test in a cold room to decide the proper film types that will be used during this study. As a result, most of the pressures were detected between 2.5MPa to 70MPa pressure range and only the small portion of the high pressure was captured. Therefore, only three types of pressure film (low, medium, and high) were adopted in this study. Table 1 represents the pressure ranges of each film type.

Table 1. Pressure range of pressure film type

Film type	Pressure range (MPa)
Low	2.5 - 10
Medium	10 - 50
High	50 – 130

There are two types of pressure measurement film, 1) 'Mono-sheet' type and 2) 'Two-sheet' type. Structures of each type of pressure measurement film were illustrated in Figure 1.

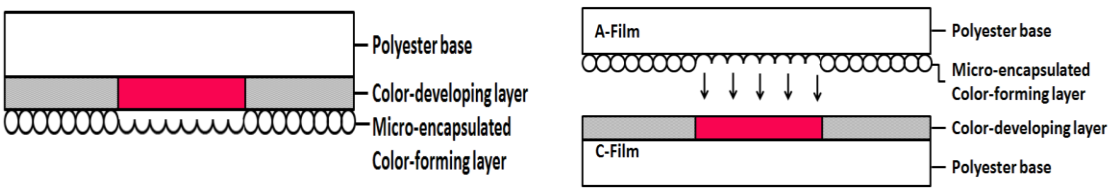

Figure 1. Structures of pressure measurement film (Left: Mono-sheet, Right: Two sheet type)

The reaction mechanism is identical in both types of films. The procedure is, 1) pressure applied on the face of pressure film, 2) micro-capsules are broken, 3) color forming material reacts with the color developing material, 4) color turns as red. The color density will represent the certain pressure level. As red density getting darker, this means that the pressure is getting higher. Each pressure measurement film is one-time use only.

TEST CONDITION

Test conditions are represented in Table 2. Cold room temperature, grain size, crushing speed, and cone angle were considered as a controlled parameter during the test.

Table 2. Test conditions

Test No.	Cold room temperature (°C)	Grain size (mm)	Crushing speed (mm/sec)	Cone angle (°)
1	-15	5 - 10	100	30
2	-15	1 - 4	1	30
3	-5	1 - 4	1	50
4	-15	5 - 10	1	50
5	-15	1 - 4	100	50
6	-5	1 - 4	100	30
7	-5	5 - 10	100	50
8	-5	5 - 10	1	30

In case of 30° cone angle sample, tests were performed in three crushing steps, and 50° cone angle was consisted of four crushing steps to measure contact area and pressure distribution at each step. Figure 2 illustrated designed penetration distance at each step.

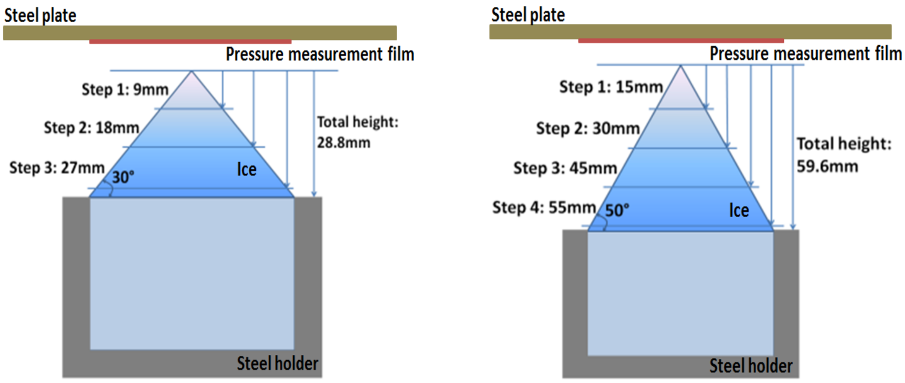

Figure 2. Designed penetration distance of each step with 30° and 50° cone angle

Low, medium, and high pressure measurement film were stacked together to obtain a variety of pressure levels at a certain film type. As a result, pressure distribution map and spatial pressure-area curve at each step were plotted using obtained data.

IMAGE PROCESSING METHOD

Procedure of image processing method was introduced by Kim and Ulan-Kvitberg [1][2]. Data from the tested pressure measurement film was obtained by following steps.

Pressure measurement film scanning

The tested pressure measurement film was scanned with 1200dpi and saved as an image file. Figure 3 shows an example of scanned pressure measurement film in low-type.

Figure 3. Scanned & saved pressure measurement film (Low-type)

Pixel value determination

Prior to proceed to pixel value determination step, saved image was opened to remove an unnecessary part of the film, such as a scratch, (source of possible error which could count as applied pressure while plotting spatial pressure-area curve) except the activated pressure pattern location. The main purpose of this pre-step is only to include the actual force which was applied on the surface. Once after the scanned pressure film is cleaned, pixel size was properly controlled and converted to 16-bit image. Pixel values were recorded to a text file by xy coordinates (xy represents a pixel location) and z-value in the active image.

Pressure value conversion

Obtained 'Z-value' from the previous step was converted to the practical pressure value at a certain xy pixel location using regression equation obtained from calibration test. Three types of pressure measurement film were converted for each image, and only the maximum pressure values were chosen at each xy pixel location by Microsoft Excel® software. As a result, pressure distribution map at each step was plotted.

RESULTS

In this study, four assessment items which are 'activated area', 'total force', 'spatial pressure-area curve', and 'pressure distribution map' were chosen and compared by each five different unit pixel size (5.0, 2.5, 1.0, 0.5, and 0.25mm) as a comparison purpose. The results were explained for each step and two graphs that represented max./min. deviation were presented.

Step 1: Activated area

Test 7 showed the max. deviation (17.9%) about 40mm^2 variations in an activated area. Otherwise, test 4 showed min. deviation (1.8%) about 10mm^2 variations.

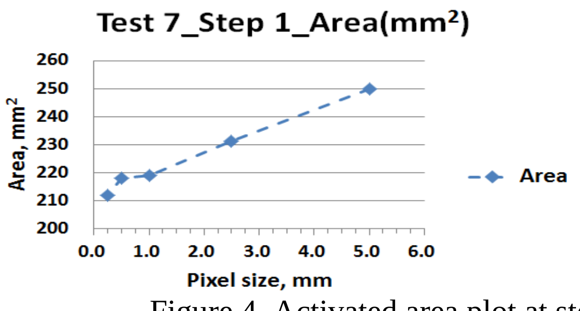

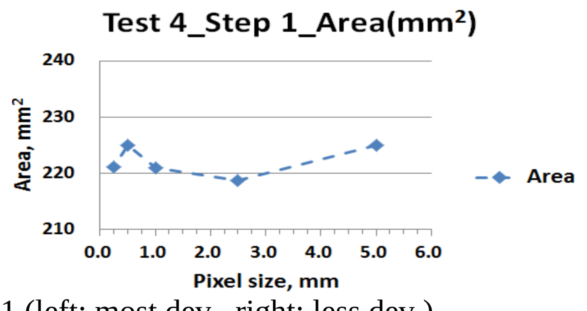

Figure 4. Activated area plot at step 1 (left: most dev., right: less dev.)

Table 3 represents results of all activated area by each pixel size at step 1. Value in a parenthesis indicates the relative proportions for the 0.25mm pixel size. '+' sign indicates that the obtained value showed over-estimation. In contrast, '-' sign indicates that the obtained value showed under-estimation. The acceptable error range is set within ±5%, marked in red represents that obtained value was out of range by selected error range.

Results were obtained for all pixels within the acceptable range in test 3 and 4. On the other hand, all values in test 6 were out of the acceptable range. From the table 1, the results indicated that error range was increased as the pixel size getting larger. Approximately, 38% of obtained results showed greater than ±5% error range. If acceptable error range is expanded within ±10%, the percentage of 'out of range' results decreased as 6%.

Table 3. Results of activated area: Step 1

Pixel size (mm)	Test 1	Test 2	Test 3	Test 4	Test 5	Test 6	Test 7	Test 8
5.0	500.00 (7.0)	475.00 (-8.2)	275.00 (-3.4)	225.00 (1.8)	225.00 (4.0)	675.00 (8.0)	250.00 (17.9)	250.00 (13.6)
2.5	462.50 (-1.0)	500.00 (-3.4)	275.00 (-3.4)	218.75 (-1.1)	231.25 (6.9)	687.50 (10.0)	231.25 (9.0)	225.00 (2.2)
1.0	472.00 (1.0)	513.00 (-0.9)	275.00 (-3.4)	221.00 (-0.1)	230.00 (6.3)	663.00 (6.1)	219.00 (3.2)	229.00 (4.1)
0.5	475.00 (1.7)	514.50 (-0.6)	279.75 (-1.7)	225.00 (1.8)	226.50 (4.7)	664.25 (6.3)	218.00 (2.8)	233.50 (6.1)
0.25	467.25	517.44	284.56	221.13	216.31	624.94	212.13	220.06

Step 1: Total force

Test 8 showed the max. deviation (24%) about 1.4kN variation in total force result. Otherwise, test 3 showed min. deviation (3.1%) about 0.23kN variation.

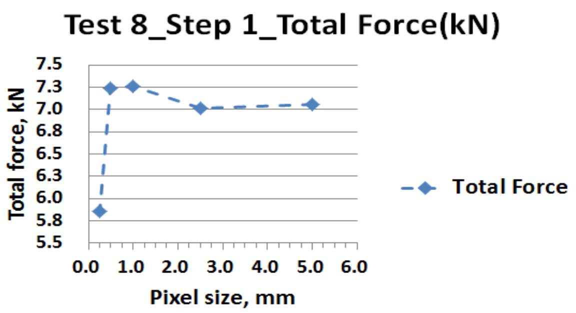

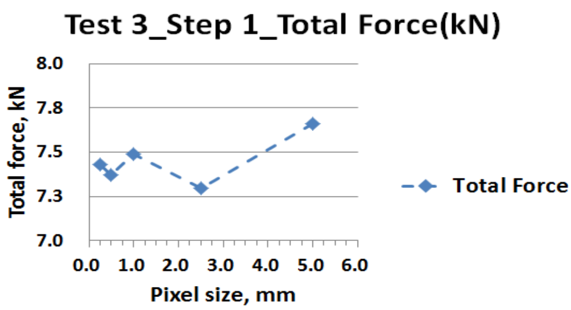

Figure 5. Total force plot at step 1 (left: most dev., right: less dev.)

Table 4 showed that the relative proportions for the 0.25mm pixel size showed greater differences in total force compared to an activated area. All the results of test 1,2,4,7, and 8 represent over ±5% error range and only the test 3 satisfied the error criteria. Results of total forces showed a significant deviation compared to an activated area. Approximately, 78% of obtained results showed greater than ±5% error range. If acceptable error range is expanded to ±10% error range, percentage of 'out of range' results decreased as 44%.

Table 4. Results of total force: Step 1

Pixel size (mm)	Test 1	Test 2	Test 3	Test 4	Test 5	Test 6	Test 7	Test 8
5.0	18.62 (27.8)	16.19 (8.8)	7.66 (3.1)	6.19 (12.3)	4.81 (3.0)	13.61 (-0.1)	6.21 (11.0)	7.06 (20.7)
2.5	16.41 (12.6)	16.00 (7.5)	7.30 (-1.8)	6.78 (23.0)	4.95 (5.9)	13.91 (2.0)	6.33 (13.0)	7.02 (19.8)
1.0	15.94 (9.4)	16.15 (8.5)	7.49 (0.7)	6.28 (13.9)	5.11 (9.4)	14.98 (9.9)	5.99 (7.0)	7.26 (24.0)
0.5	15.85 (8.8)	16.07 (8.0)	7.37 (-0.8)	6.35 (15.2)	5.05 (8.0)	15.01 (10.1)	6.23 (11.4)	7.24 (23.7)
0.25	14.57	14.89	7.43	5.51	4.67	13.63	5.60	5.85

Step 1: Pressure distribution

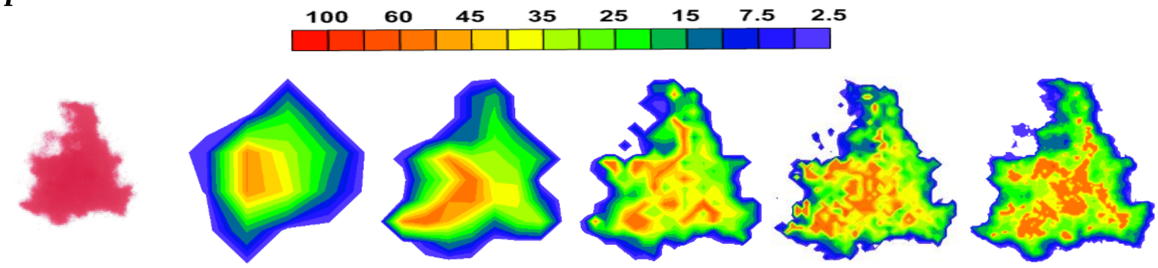

(a) pattern (b) 5.0mm (c) 2.5mm (d) 1.0mm (e) 0.5mm (f) 0.25mm

Figure 6. Pressure distribution at step 1 (Test 7)

Figure 6 shows the pressure distribution in step 1. Figure 6 (a) represents an original pressure image of step 1 in test 7 (only low type film). Normally, low film captures the most patterns through the test (low film will capture any pattern even applied pressure is greater than 10 MPa). Figure 6 (b) to (f) shows the pressure distribution at each pixel size. It is easy to recognize that finer pixel size will give more detailed distribution compare to coarse pixel size. However, 1.0mm pixel size showed a sufficient outline of pressure distribution.

Step 1: Spatial pressure-area curve

Spatial pressure-area curve was plotted by 'Contour-averaging' method, which was suggested by Kim [1]. Figure 7 showed that the variance between each pixel size was significant in test 4. In contrast, pressure-area curve in test 3 was almost identical in each pixel size.

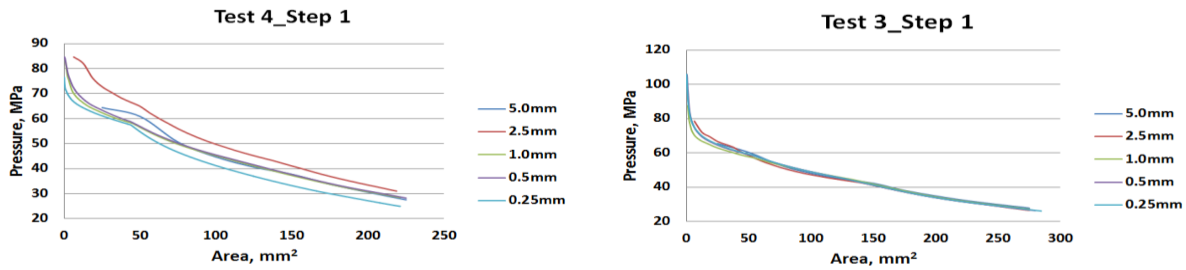

Figure 7. Spatial pressure-area curve at step 1 (left: most dev., right: less dev.)

Step 2: Activated area

As shown in Table 5, greater than ±5% error range was decreased as 21% (compare to step 1). Most of the test results showed good agreement except test 4.

Table 5. Results of activated area: Step 2

Pixel size (mm)	Test 1	Test 2	Test 3	Test 4	Test 5	Test 6	Test 7	Test 8
5.0	1900.0 (-1.3)	2375.0 (2.7)	1200.0 (-2.5)	1000.0 (9.3)	1525.0 (5.9)	2150.0 (9.8)	1000.0 (-10.6)	1200.0 (4.0)
2.5	1900.0 (-1.3)	2243.8 (-3.0)	1225.0 (-0.4)	968.75 (5.9)	1418.8 (-1.4)	1987.5 (1.5)	1081.3 (-3.3)	1106.3 (-4.1)
1.0	1917.0 (-0.4)	2284.0 (-1.2)	1224.0 (-0.5)	970.00 (6.0)	1407.0 (-2.2)	1994.0 (1.8)	1093.0 (-2.3)	1118.0 (-3.1)
0.5	1920.8 (-0.2)	2263.0 (-2.1)	1231.8 (0.1)	968.25 (5.8)	1409.5 (-2.1)	1999.8 (2.1)	1103.0 (-1.4)	1126.0 (-2.4)
0.25	1924.5	2312.4	1230.4	914.94	1439.4	1958.3	1118.6	1153.7

The percentage of ‘out of range’ decreased to compare to step 1. As activated area getting larger, source of error diminished, which means accuracy is tended to be positive.

Step 2: Total force

Results of total forces showed large deviations as similar to the step 1 (72% with greater than ±5% error range and 41% with greater than ±10% error range). In case of test 1,4,5,6, and 7, all of the test results showed over ±5% error range. Especially, excessive variation was observed in test 7, over 25%.

Table 6. Results of total force: Step 2

Pixel size (mm)	Test 1	Test 2	Test 3	Test 4	Test 5	Test 6	Test 7	Test 8
5.0	36.01 (10.7)	44.70 (1.1)	17.68 (-4.2)	24.51 (-15.3)	12.82 (5.1)	16.18 (8.3)	22.85 (34.6)	15.90 (0.3)
2.5	36.12 (11.1)	45.86 (3.8)	17.77 (-3.7)	30.48 (5.3)	13.26 (8.7)	16.79 (12.4)	21.54 (26.9)	17.04 (7.4)
1.0	35.98 (10.6)	46.25 (4.7)	18.45 (-0.1)	31.84 (10.0)	13.22 (8.4)	16.57 (10.9)	21.45 (26.3)	17.16 (8.2)
0.5	36.15 (11.1)	46.26 (4.7)	18.41 (-0.2)	31.51 (8.9)	13.33 (9.3)	16.74 (12.0)	21.41 (26.1)	17.25 (8.8)
0.25	32.52	44.19	18.46	28.94	12.20	14.94	16.98	15.86

As represented in Table 6, the conflicting result was observed (as pressure pattern getting larger, the accuracy of the activated area was increased). However, even pattern getting larger, the accuracy of total forces remained similar compared to step 1. This means that larger pressure pattern will not always guarantee the accuracy of the results.

Step 2: Pressure distribution

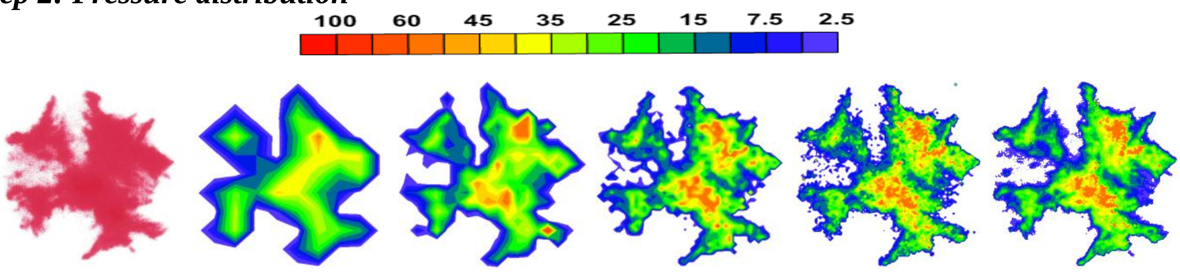

(a) pattern (b) 5.0mm (c) 2.5mm (d) 1.0mm (e) 0.5mm (f) 0.25mm

Figure 8. Pressure distribution at step 2 (Test 7)

Figure 8 shows the pressure distribution in step 2. As similar to Figure 6, Figure 8 (a) represents an original pressure image of step 2 in test 7 (only low type film). Figure 8 (b) to (f) shows a pressure distribution map at each pixel size. As mentioned earlier, it is easy to recognize that finer pixel size will give more detailed distribution compare to coarse pixel size. In Figure 8, general outline of pressure distribution with 5.0mm was quite different from the others. However, similar pattern for the pixel size of 5.0mm was observed in step 2 even the overall shape was somewhat rough.

Step 2: Spatial pressure-area curve

In step 2, spatial pressure-area curve showed good agreement in most tests. In test 4, trend of curves showed a similar trend except 5.0mm pixel size (quite offset). In test 3, trend of curves were almost identical from the initial point.

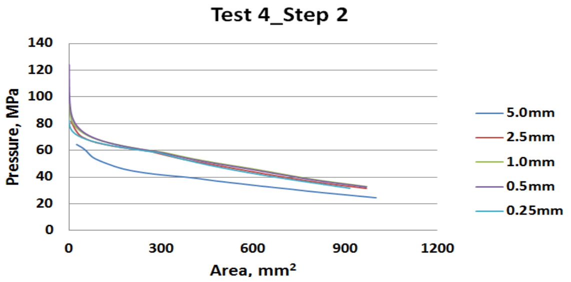

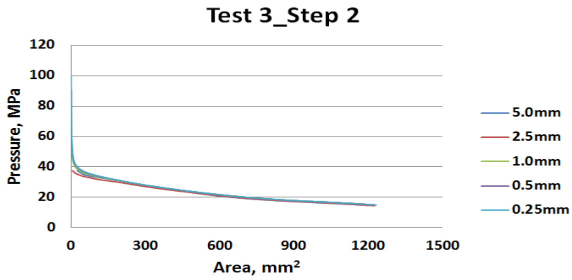

Figure 9. Spatial pressure-area curve at step 2 (left: most dev., right: less dev.)

Step 3: Activated area

As shown in Table 7, percentage of greater than ±5% error range was similar to step 2 (25%). Most of the test results showed good agreement except test 1 and 7.

Table 7. Results of activated area: Step 3

Pixel size (mm)	Test 1	Test 2	Test 3	Test 4	Test 5	Test 6	Test 7	Test 8
5.0	4275.0 (-2.2)	3550.0 (0.3)	3225.0 (1.7)	1675.0 (-2.4)	3675.0 (-4.9)	3550.0 (-5.9)	1900.0 (-0.5)	3025.0 (-2.1)
2.5	4043.8 (-7.5)	3518.8 (-0.6)	3137.5 (-1.1)	1650.0 (-3.8)	3668.8 (-5.1)	3643.8 (-3.4)	1812.5 (-5.1)	3000.0 (-2.9)
1.0	4113.0 (-5.9)	3482.0 (-1.6)	3157.0 (-0.5)	1699.0 (-1.0)	3686.0 (-4.7)	3619.0 (-4.1)	1802.0 (-5.6)	2979.0 (-3.5)
0.5	4096.8 (-6.3)	3507.3 (-0.9)	3165.0 (-0.2)	1681.8 (-2.0)	3696.8 (-4.4)	3584.5 (-5.0)	1784.5 (-6.6)	2983.5 (-3.4)
0.25	4370.1	3539.4	3172.6	1715.9	3865.9	3773.3	1909.9	3088.6

Step 3: Total force

Results of total forces in step 3 showed similar trends compare to previous step 1 and 2 (72% with ±5% error range). The overall results of total force were not improved.

Table 8. Results of total force: Step 3

Pixel size (mm)	Test 1	Test 2	Test 3	Test 4	Test 5	Test 6	Test 7	Test 8
5.0	45.70 (9.0)	49.84 (17.0)	36.86 (2.8)	27.50 (0.9)	41.71 (10.3)	53.36 (9.4)	30.36 (-2.6)	36.63 (0.5)
2.5	44.36 (5.8)	47.40 (11.2)	35.58 (-0.8)	29.34 (7.7)	41.35 (9.4)	55.46 (13.7)	32.14 (3.1)	38.85 (6.6)
1.0	44.75 (6.8)	47.22 (10.8)	35.58 (0.0)	29.29 (7.5)	41.25 (9.1)	53.85 (10.4)	32.80 (5.2)	39.92 (9.5)
0.5	44.45 (6.1)	46.96 (10.2)	35.70 (-0.4)	29.65 (8.8)	41.29 (9.2)	53.77 (10.2)	33.30 (6.8)	39.47 (8.3)
0.25	41.91	42.61	35.85	27.25	37.81	48.79	31.17	36.45

However, a percentage of variation was decreased approximately less than half (44% -> 25%) when the acceptable range is extended to 10%.

Step 3: Pressure distribution

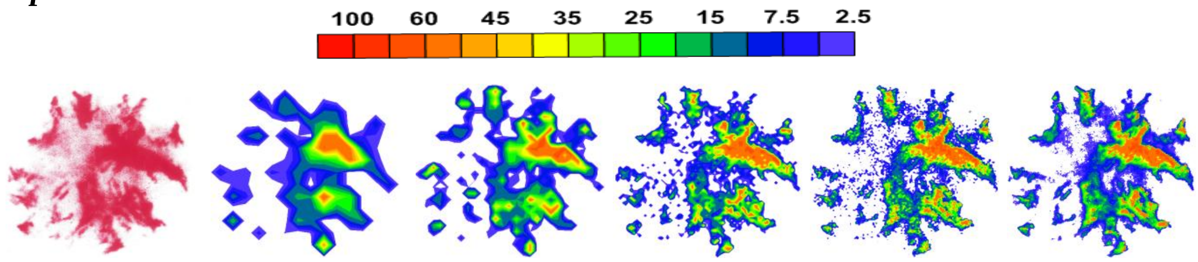

(a) pattern (b) 5.0mm (c) 2.5mm (d) 1.0mm (e) 0.5mm (f) 0.25mm

Figure 10. Pressure distribution at step 3 (Test 7)

Figure 10 shows the pressure distribution in step 3. As illustrated in Figure 10, it was possible to figure out the overall outline of pressure distribution with 5.0mm pixel size. However, detailed pressure distribution was well described after 1.0mm pixel size.

Step 3: Pressure-Area curve

Spatial pressure-area curve becomes similar as step progress as represented in Figure 11.

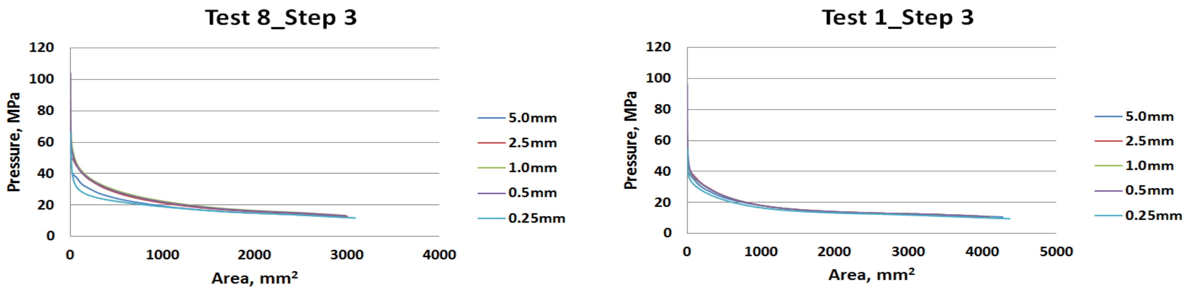

Figure 11. Spatial pressure-area curve at step 3 (left: most dev., right: less dev.)

Step 4: Activated area/Total force/Spatial pressure-area curve

Results of an activated area were slightly decreased to compare to step 3 (25% -> 19%). However, overall results of total force were maintained over the steps (over 70%). This means that total force is normally tended to be overestimated according to a pixel size.

Table 9. Results of activated area/total force: Step 4

	Activated area				Total force			
Pixel size (mm)	Test 3	Test 4	Test 5	Test 7	Test 3	Test 4	Test 5	Test 7
5.0	5625.0 (-0.7)	2675.0 (-2.9)	5575.0 (-4.6)	3675.0 (1.1)	68.46 (4.2)	26.75 (25.1)	67.79 (6.3)	57.33 (13.0)
2.5	5606.3 (-1.0)	2550.0 (-7.5)	5618.8 (-3.9)	3712.5 (2.2)	66.15 (0.7)	25.53 (19.3)	67.37 (5.7)	56.73 (11.8)
1.0	5671.0 (0.1)	2505.0 (-9.1)	5573.0 (-4.6)	3679.0 (1.2)	65.61 (-0.1)	24.82 (16.1)	67.04 (5.1)	54.27 (7.0)
0.5	5673.3 (0.2)	2529.3 (-8.2)	5583.8 (-4.5)	3675.8 (1.2)	65.58 (-0.2)	24.84 (16.1)	67.06 (5.2)	54.11 (6.7)
0.25	5663.4	2756.1	5844.6	3633.0	65.70	21.39	63.76	50.73

The trends of spatial pressure-area curve and pressure distribution showed similar results in step 4. As the test processed, the overall results, which are activated area, spatial pressure-area curve, and pressure distribution, represented good agreement except total force.

CONCLUSIONS AND RECOMMENDATION

In this study, high-resolution pressure measurement film was applied in laboratory ice crushing test to explore a realistic pattern of contact area and pressure distribution during the ice crushing test in a laboratory.

Different pixel size was chosen for the data analysis in order to assess the effect of the pixel size to the results. Four assessment categories were selected and analyzed and as a result,

1) Activated area: effect of pixel size was slightly decreased as the test step was processed. Based on the analysis, pixel size below 2.5mm is expected to provide good agreement compared to 0.25mm pixel size.

2) Total force: percentage of 'out of range' was normally over 70% in every step. This represents that total force is highly sensitive to pixel size and tend to overestimate the total force in general.

3) Spatial pressure-area curve: represented similar trends throughout the tests/steps.

4) Pressure distribution: sufficient to identify the general outline of the pattern with 5.0mm pixel size after step 1. Smaller pixel size provided more detailed distribution of pressure, however, 1. 0mm pixel size showed good agreement in terms of a detailed plot.

It was unable to reach a conclusion whether unconditionally smaller pixel size is always better for precise data analysis. In addition, it was also unable to conclude that whether the larger pixel is better for efficient data analysis. As shown previously, the sensitivity by the pixel size was varied from each test cases and assessment categories. Therefore, sensitivity of data analysis by varying the pixel size need to be more carefully evaluated.

Furthermore, the result of this study was solely analyzed by relative comparison based on 0.25mm pixel size. This means that there is possibility that the results may differ if the analysis is performed to the smaller pixel size than 0.25mm. Therefore, the future study will be useful for the evaluation of data analysis using a pixel size smaller than 0.25mm to evaluate/confirm the overall trend from this study.

ACKNOWLEDGEMENTS

Financial support for this study was provided by the 'STePS^2' (Sustainable Technology for Polar Ships & Structures) project. And particular thanks to Craig Mitchell for assistance in conducting the tests in cold room.

REFERENCES

[1] Kim, H., Daley, C., and Ulan-Kvitberg, C., 2012. Reappraisal of Pressure Distribution Induced by Ice-Structure Interaction Using High-Precision Pressure Measurement Film. ICETECH 2012, Banff, Canada

[2] Ulan-Kvitberg, C.A., 2012. Adapting Pressure Films to Measure Pressure Patterns in Ice-Steel Interaction Experiments. Masters thesis, Memorial University of Newfoundland, Canada

[3] Daley, C., 2004. A Study of the Process-Spatial Link in Ice Pressure-Area Relationships. NRC PERD/CHC Report 7-108

[4] Golden Software, "Surfer 11", [Online]. Available: http://www.goldensoftware.com/products/ surfer.shtml [Accessed 4 January 2013]